

# Nuclear Translocation of $\beta$ -Catenin Mediates the Parathyroid Hormone-Induced Endothelial-to-Mesenchymal Transition in Human Renal Glomerular Endothelial Cells

Min Wu, Ri-Ning Tang, Hong Liu, Kun-Ling Ma, Lin-Li Lv, and Bi-Cheng Liu\*

*Institute of Nephrology, Zhongda Hospital, Southeast University School of Medicine, Nanjing, China*

## ABSTRACT

Emerging evidence shows that increased parathyroid hormone (PTH) accelerates endothelial injury and subsequent organ fibrosis. Although the underlying mechanisms remain largely unknown, the endothelial-to-mesenchymal transition (EndMT) has recently been demonstrated to be a crucial event during fibrotic disorders. Therefore, the present study aimed to investigate whether elevated PTH could induce EndMT in primary human renal glomerular endothelial cells (GECs) and to determine the possible underlying signaling pathway. The expression of EndMT-related markers was determined by real-time PCR, Western blotting, and confocal microscopy. The results showed that PTH receptor (PTHrP) was expressed in GECs and its expression was decreased by increasing concentration of PTH. Moreover, PTH significantly inhibited the expression of endothelial marker CD31 and increased the expression of mesenchymal markers FSP1 and  $\alpha$ -SMA in concentration- and time-dependent manners. Confocal microscopy revealed an increasing overlap of CD31 with FSP1 in some GECs after PTH treatment. The expression of type I collagen was upregulated by PTH. Furthermore, PTH enhanced the nuclear  $\beta$ -catenin protein levels, and decreased cytoplasmic  $\beta$ -catenin expression in GECs was observed. In contrast, DKK1, an inhibitor of  $\beta$ -catenin nuclear translocation, attenuated such changes in EndMT-related markers induced by PTH. In summary, these data demonstrated that elevated PTH-induced EndMT in human GECs might be partially mediated by the nuclear translocation of  $\beta$ -catenin. *J. Cell. Biochem.* 115: 1692–1701, 2014. © 2014 Wiley Periodicals, Inc.

**KEY WORDS:** PARATHYROID HORMONE; GLOMERULAR ENDOTHELIAL CELL; ENDOTHELIAL-TO-MESENCHYMAL TRANSITION;  $\beta$ -CATENIN; DKK1

Renal fibrosis is a common final pathway for almost all progressive chronic kidney disease (CKD) [Liu, 2011]. Numerous studies have focused on the roles of podocytes, mesangial cells and the glomerular basement membrane in the pathogenesis of renal fibrosis [Jefferson et al., 2011; Greka and Mundel, 2012], whereas the importance of glomerular endothelial cells (GECs) has been largely ignored. Recently, experimental studies have shown that GEC injury initiates and propels the development and progression of glomerulopathy and renal fibrosis in animal models with CKD [Nakagawa et al., 2007; Nagasu et al., 2012; Sun et al., 2013]. In addition, clinical investigations have also provided correlations between the loss of glomerular endothelial cells and the exacerbation of renal dysfunction [Landray et al., 2004; Theilade et al., 2012; Weil et al., 2012; Grutzmacher et al., 2013]. Collectively, these findings strongly suggest the crucial role of glomerular endothelial injury in the progression of renal fibrosis.

Glomerular endothelial alterations could be caused by a number of pathologic processes mediated by mechanical, inflammatory and oxidative stress-associated factors [Jaimes et al., 2010; Bevan et al., 2011; Izawa-Ishizawa et al., 2012]. Elevated parathyroid hormone (PTH) levels are common in patients with CKD. Although the importance of PTH in mineral metabolism is well recognized, recent studies suggest that PTH could directly induce endothelial dysfunction and contribute to organ fibrosis [Rashid et al., 2007a,b; 2008; Loncar et al., 2011]; nevertheless, the underlying mechanisms remain largely unknown. As the endothelial-to-mesenchymal transition (EndMT) has been demonstrated to be important for the development of endothelial dysfunction and subsequent fibrotic disorders [Zeisberg et al., 2007; 2008; Li et al., 2009; Hashimoto et al., 2010; Rieder et al., 2011; Tang et al., 2013], we hypothesized that elevation of PTH could promote EndMT in GECs. In the present study, we investigated the effect of PTH on EndMT in cultured

Author's information: Ri-Ning Tang as co-first author.

No conflicts of interest, financial or otherwise, are declared by the authors.

Grant sponsor: National Natural Science Foundation of China (Key Program); Grant numbers: 81130010, 81370919; Grant sponsor: Natural Science Foundation of Jiangsu Province; Grant numbers: BK 2011603, BK 2012751.

\*Correspondence to: Bi-Cheng Liu, MD, PhD, Institute of Nephrology, Zhongda Hospital, Southeast University, Nanjing 210009, China. E-mail: liubc64@163.com

Manuscript Received: 18 October 2013; Manuscript Accepted: 8 May 2014

Accepted manuscript online in Wiley Online Library (wileyonlinelibrary.com): 12 May 2014

DOI 10.1002/jcb.24832 • © 2014 Wiley Periodicals, Inc.

primary human GECs and the molecular pathway that may be involved.

## MATERIALS AND METHODS

### CELL CULTURE AND TREATMENT

Primary human renal GECs were purchased from ScienCell Research Laboratories (Carlsbad, CA) and cultured according to the manufacturer's protocol. Briefly, cells were grown in endothelial culture medium (ScienCell) containing 5% fetal bovine serum (FBS) (ScienCell), 1% endothelial cell growth supplement (ScienCell) and 1% penicillin/streptomycin solution (ScienCell) in 5% CO<sub>2</sub> at 37°C. Passage 3–4 GECs were expanded in monolayers in flasks or dishes.

At approximately 80% confluence, the culture medium was changed to a serum-free solution for 24 h prior to their use in all experiments. Human recombinant PTH fragment 1–34 (Sigma, USA) was used, and dickkopf 1 (DKK1) (Peprotech, USA) was then added to the serum-free medium. All experiments for this study were performed at least in triplicate.

### REAL-TIME PCR

Total RNA was extracted using RNAiso Plus according to the manufacturer's directions (TAKARA, China). The RNA concentration and purity were confirmed with a Nanodrop 2000 (Thermo, USA). Samples with a relative absorbance ratio at 260/280 between 1.8 and 2.0 were used. All RNA samples were reverse transcribed (Applied

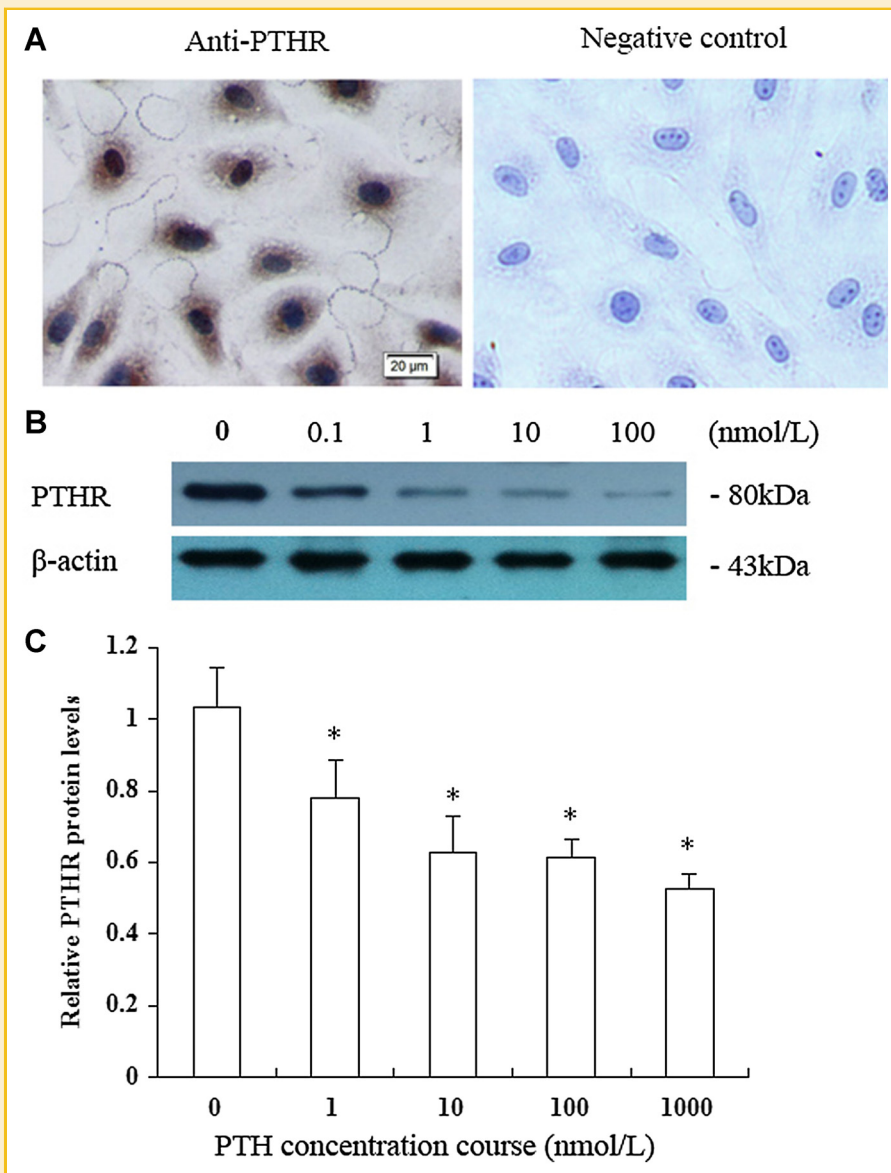


Fig. 1. Expression of PTHR in GECs. A: Immunocytochemical staining of PTHR in GECs. Brown staining in the cell indicates the presence of PTHR. Scale bar, 20  $\mu$ m. B,C: GECs were incubated for 48 h with increasing concentrations of PTH (0–100 nmol/L). Representative Western blots (B) and quantitative determinations of PTHR protein levels (C) are presented. The data are expressed as the means  $\pm$  SD. \* $P$  < 0.05 versus 0 group.

Biosystems, USA). The quantification of specific mRNAs was carried out using an ABI Prism 7300. Sequence Detection System (Applied Biosystems, USA) with the SYBR Green Real-time PCR Kit (TAKARA, China). The following oligonucleotide primer sequences were used: CD31: forward 5'-GAGTCCAGCCGCATATCC-3', reverse 5'-TGACA-CAATCGTATCTTCTC-3'; FSP1: forward 5'-GTCCACCTTCCA-CAAGTAC-3', reverse 5'-TGCCAAGTTGCTCATCAG-3;  $\alpha$ -SMA: forward 5'-GACAATGGCTCTGGGCTCTGTAA-3', reverse 5'-ATGC-CATGTTCTATCGGGTACTTCA-3'; type I collagen: forward 5'-

CGATGGATTCCAGTTCGAGTATG-3', reverse 5'-TGTTCTTGCACT-GGTAGGTGATG-3';  $\beta$ -actin: forward 5'-CTGGAAGGTGGACAGC-GAGG-3', reverse 5'-TGACGTGGACATCCGCAAAG-3' (designed and synthesized by Genaray, China). The relative amount of mRNA was normalized to  $\beta$ -actin and calculated using the standard curve method. In brief, the pre-PCR product of each gene was used as the standard. The standard curve was established with a 10-fold serial dilution of the product and was included in all PCR runs. The ratio of target gene abundance/housekeeping gene abundance was

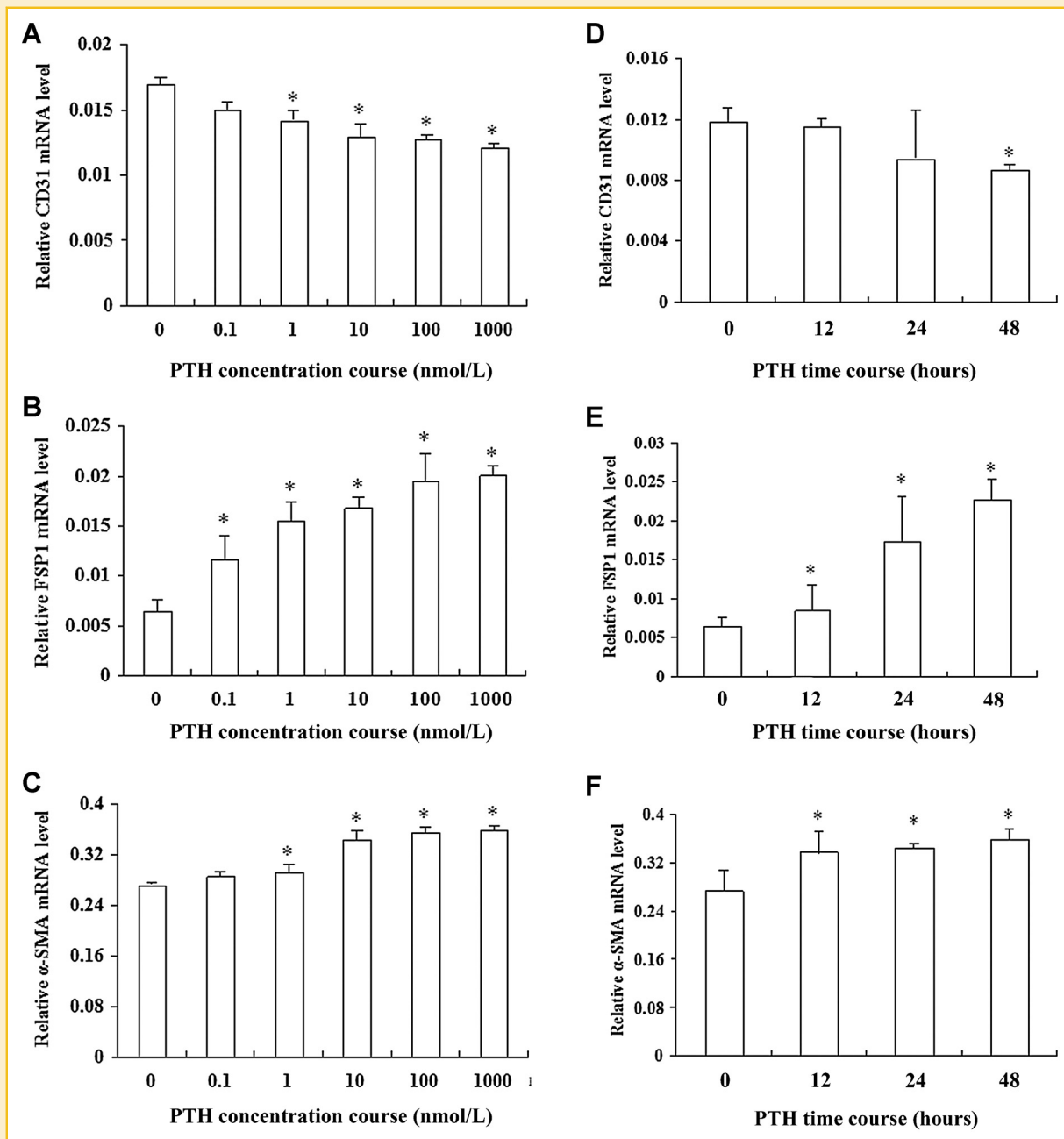


Fig. 2. Effect of PTH on mRNA expression of CD31, FSP1 and  $\alpha$ -SMA in GECs. A–C: GECs were incubated for 48 h with increasing concentrations of PTH (0–1,000 nmol/L). D–F: GECs were incubated with PTH (100 nmol/L) for different periods (0–48 h) as indicated. The mRNA expressions were assessed by real-time PCR. The data are expressed as the means  $\pm$  SD. \* $P < 0.05$  versus 0 group.

used to evaluate the expression level of each gene. Controls consisting of ddH<sub>2</sub>O were negative in all runs.

### WESTERN BLOTTING

Total, cytoplasmic and nuclear proteins were prepared using the Total Protein Extraction Kit and Nuclear and Cytoplasmic Protein

Extraction Kit, respectively (KeyGen, China). Protein concentrations were measured using a protein assay kit (KeyGEN, China). Equal amount of the protein obtained from each lysate was electrophoresed in a 4–20% SDS–polyacrylamide gel and transferred onto nitrocellulose membrane (Pall, USA) by electroblotting. The blots were incubated overnight with primary antibodies against

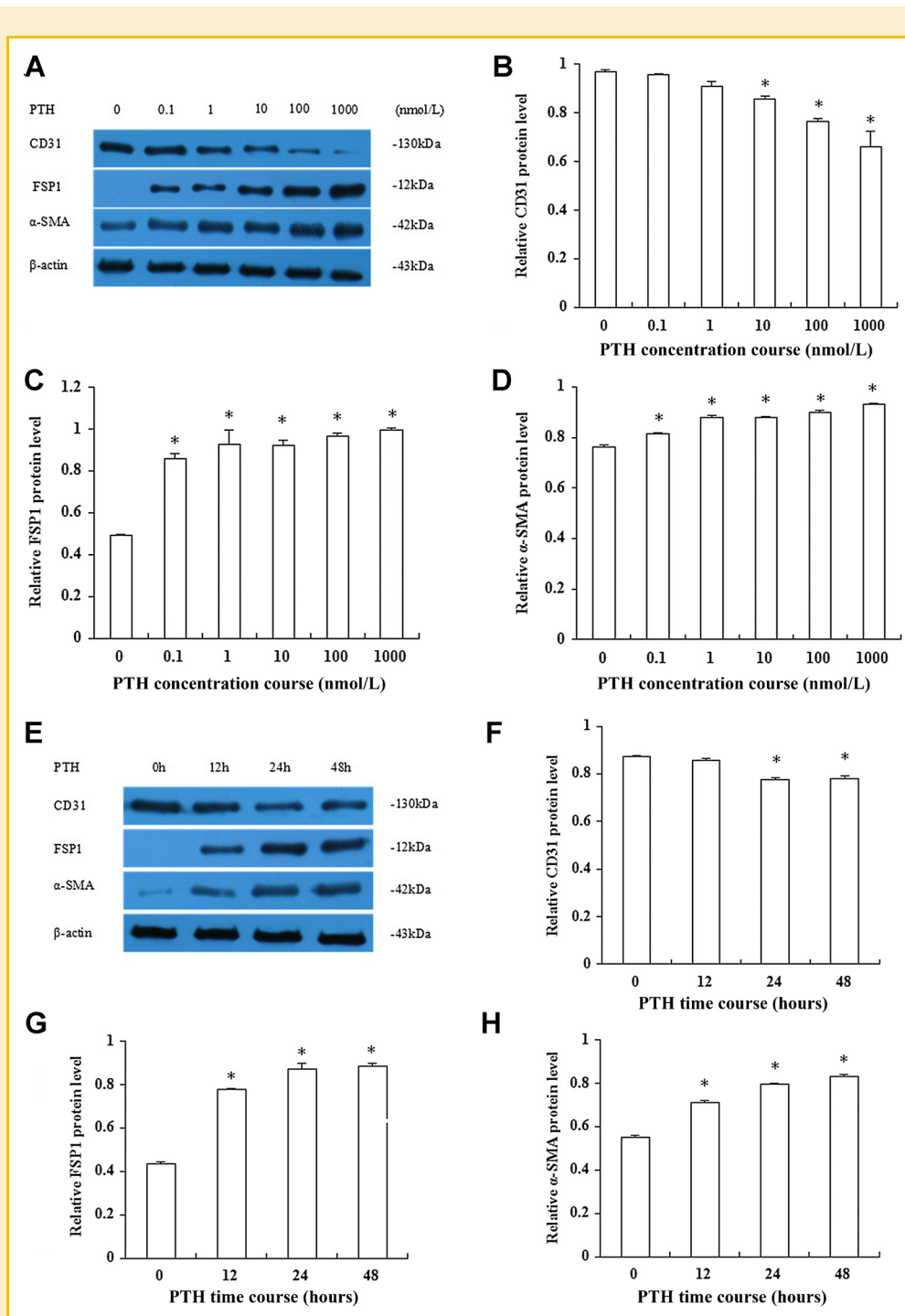


Fig. 3. Effect of PTH on protein expression of CD31, FSP1 and α-SMA in GECs. A–D: GECs were incubated for 48 h with increasing concentrations of PTH (0–1,000 nmol/L). E–H: GECs were incubated with PTH(100 nmol/L) for different periods (0–48 h) as indicated. Protein expressions were assessed by Western blotting. The data are expressed as the means ± SD. \**P* < 0.05 versus 0 group.

CD31 (sc-1506, Santa Cruz, CA), FSP1 (ab-27957, Abcam, Hong Kong),  $\alpha$ -SMA (ab-5694, Abcam), type I collagen (ab-292, Abcam), PTH receptor (PTHr) (sc-20749, Santa Cruz) and  $\beta$ -catenin (sc-7199, Santa Cruz) followed by horseradish peroxidase-labeled secondary IgG (Santa Cruz). The signals were detected using an advanced ECL system (GE Healthcare, UK).  $\beta$ -actin and lamin-B were used as the internal controls for total and nuclear proteins, respectively.

#### IMMUNOFLUORESCENCE STAINING

GECs grown on coverslips were fixed with 4% paraformaldehyde, permeabilized with 0.1% Triton X-100, blocked with 10% bovine serum albumin (BSA) in phosphate-buffered saline at room temperature. The slides were then immunostained with primary antibodies against CD31 (sc-1506), FSP1 (ab-27957) and  $\beta$ -catenin (sc-7199) at 4°C overnight. After incubated with secondary antibodies for 1 h at room temperature in the dark, images were captured using a laser scanning confocal microscope (LSM 510 META, Zeiss, Germany).

#### IMMUNOCYTOCHEMICAL STAINING

Immunohistochemical staining was performed using the routine protocol. The primary antibody used was PTHr (sc-20749). For the negative controls, the specific primary antibody was replaced with phosphate-buffered saline.

#### TRANSMISSION ELECTRONIC MICROSCOPY (TEM)

Cells were fixed in 2.5% glutaraldehyde buffer (pH 7.4). Transmission electron microscopy (TEM) was performed according to a routine fixation and embedding procedure. Thin sections were cut on a microtome, placed on copper grids, stained with uranyl acetate and

lead citrate, and examined using a transmission electron microscope (JEM-1010, JEOL, Japan).

#### STATISTICAL ANALYSIS

Data are expressed as mean  $\pm$  standard deviation (SD). Statistical analyses were performed by one-way ANOVA using SPSS 16.0 statistical software. All *P* values were two-tailed, and *P* < 0.05 was considered to be statistically significant.

## RESULTS

#### THE EXPRESSION OF PTHR ON CULTURED HUMAN GECs

Immunocytochemical staining by PTHr antibody showed that GECs express PTHr on cell membrane and in cytoplasm (Fig. 1A). We next examined the expression of PTHr after PTH treatment. Because PTH (1–34) is the shortest fragment with the same biological activity of intact PTH, commercially available human recombinant PTH (1–34) was used to stimulate GECs [Rashid et al., 2007a, 2008]. As shown in Figure 1B,C, the PTHr protein expression was confirmed by Western blot and has been indicated to be dose dependently down-regulated in the presence of PTH.

#### PTH INDUCES EndMT IN CULTURED HUMAN GECs

As shown in Figure 2A–C, PTH at concentrations of 0–1,000 nmol/L induced a significant decrease for CD31 mRNA expression and an increase for FSP1 and  $\alpha$ -SMA after treatment for 48 h. In addition, human GECs were treated with 100 nmol/L PTH for various periods of time, and the results indicated that PTH induced a significant decrease in the level of CD31 mRNA and an increase in FSP1 and  $\alpha$ -

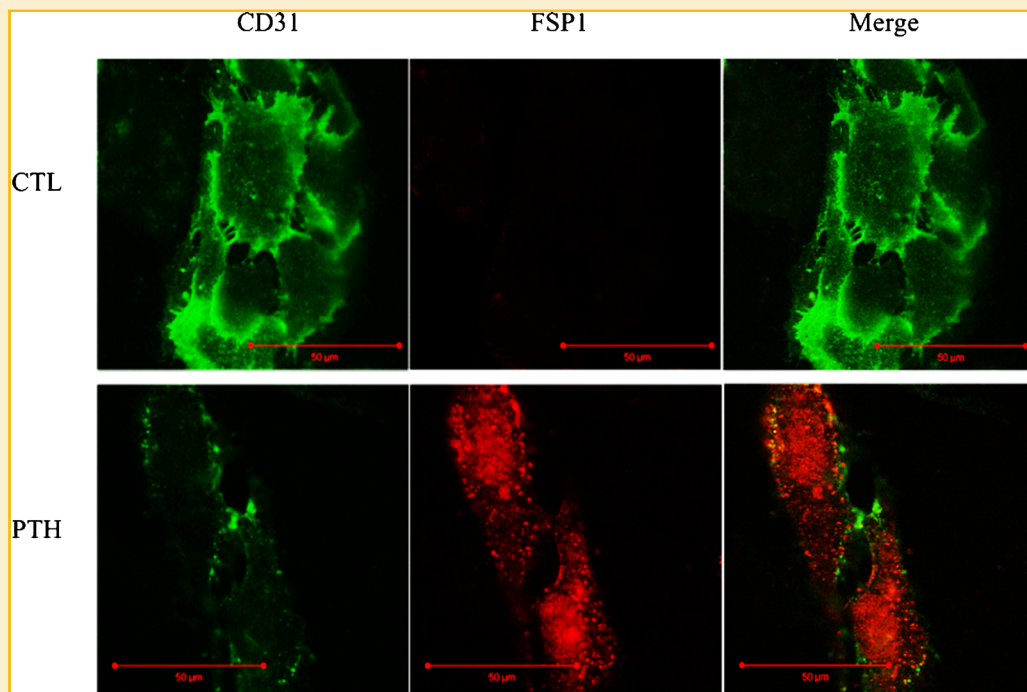


Fig. 4. The influence of PTH on immunostaining of CD31 and FSP1 in GECs. There was decreased CD31 (green) and increased FSP1 (red) staining in GECs when they were treated with 100 nmol/L PTH for 48 h. PTH, parathyroid hormone. Scale bar, 50  $\mu$ m.

SMA mRNA expression from 0 to 48 h post-treatment (Fig. 2D–F). As determined by Western blotting, PTH induced significant decreases in the protein level of CD31, a result that was accompanied by increases in the protein expression of FSP1 and  $\alpha$ -SMA in concentration- and time-dependent manners (Fig. 3). We also observed the localization of CD31 and FSP1 in GECs under confocal microscopy. As shown, GECs treated with 100 nmol/L PTH for 48 h acquired FSP1 staining and lost CD31 staining compared to the control cells (Fig. 4). We next measured the expression of type I collagen, representative extracellular matrix protein, in GECs after PTH treatment. And the result showed that PTH caused a markedly increase in the expression of mRNA and protein for type I collagen in concentration- and time-dependent manners (Fig. 5).

#### PTH INDUCES MORPHOLOGICAL CHANGES IN HUMAN GECs

As shown in Figure 6A, normal endothelial monolayers display a typical cobblestone morphology. However, some cells treated with

100 nmol/L PTH for 48 h showed a distinct change from this cobblestone-like morphology to a spindle-shaped morphology (Fig. 6A). Moreover, TEM was performed to examine the ultrastructure of the cells. The control cells displayed normal structures, whereas the cells treated with 100 nmol/L PTH for 48 h exhibited a significantly dilated endoplasmic reticulum and more vacuolization of the mitochondria (Fig. 6B). This observation indicated that GECs exposed to elevated PTH suffered from morphological changes.

#### ELEVATED PTH ACTIVATES THE NUCLEAR TRANSLOCATION OF $\beta$ -CATENIN IN HUMAN GECs

To gain further insight into the mechanisms involved in EndMT triggered by PTH in GECs, we further examined the nuclear and cytoplasmic expression of  $\beta$ -catenin in cells treated with or without PTH. As shown in Figure 7A–D, the cytoplasmic protein levels of  $\beta$ -catenin were decreased, and the nuclear protein levels of  $\beta$ -catenin

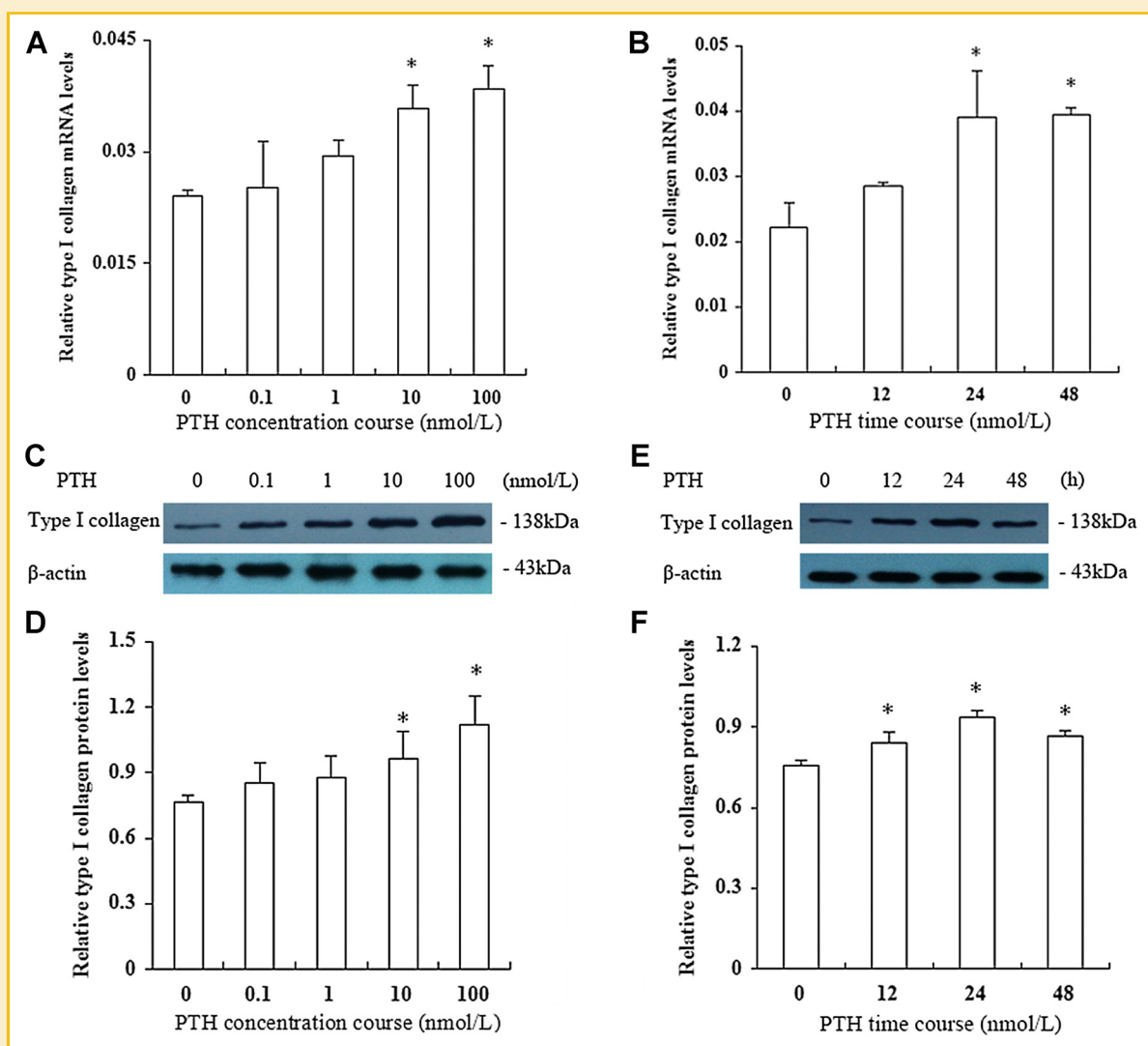
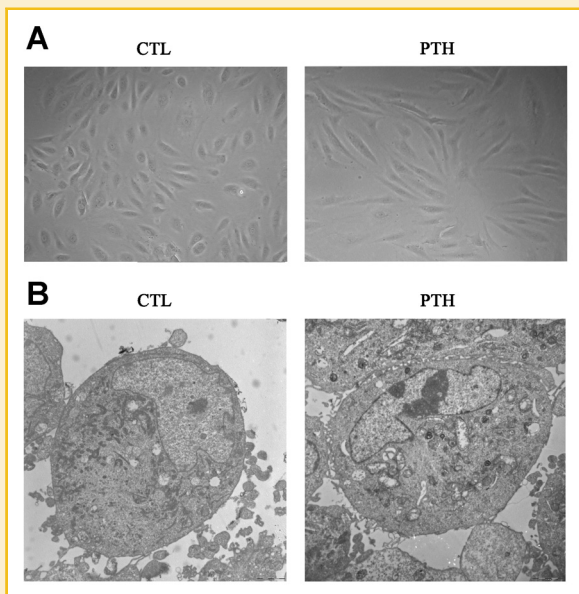


Fig. 5. Effect of PTH on the expression of type I collagen in GECs. A,C,D: GECs were incubated for 48 h with increasing concentrations of PTH as indicated. B,E,F: GECs were incubated with PTH (100 nmol/L) for different periods of time as indicated. The mRNA expression levels were determined by real-time PCR. The protein expression levels were determined by Western blot. The data are expressed as the means  $\pm$  SD. \* $P$  < 0.05 versus 0 group.



**Fig. 6.** Effect of PTH on cell morphological changes in GECs. **A:** After incubation with PTH (100 nmol/L) for 48 h, GECs lost their cobblestone feature compared with control cells (original magnification, 200 $\times$ ). **B:** TEM depicts the change in cellular ultrastructure. After PTH treatment, cells showed mitochondrial vacuolization and dilated endoplasmic reticulum (original magnification, 8,000 $\times$ ). CTL, control.

were induced in a concentration-dependent manner in GECs treated with PTH, suggesting the nuclear translocation of  $\beta$ -catenin. Moreover, immunofluorescence staining also showed a significant nuclear relocation of  $\beta$ -catenin in the cultured cells stimulated with PTH (Fig. 7E).

#### BLOCKING NUCLEAR TRANSLOCATION OF $\beta$ -CATENIN INHIBITED PTH-INDUCED EndMT IN HUMAN GECs

As a classic antagonist, DKK1 was used to block  $\beta$ -catenin nuclear translocation in vitro. There were no significant difference on expression of EndMT-related markers between cells treated with vehicle and DKK1 alone (data not shown). As shown in Figure 8, mRNA and protein expressions of CD31 were significantly upregulated in cells treated with PTH plus DKK1, when compared with cells treated with PTH alone. In contrast, administration of DKK1 largely prevented FSP1,  $\alpha$ -SMA and type I collagen expression in mRNA and protein levels. These results suggest that EndMT triggered by PTH might be partially mediated by nuclear translocation of  $\beta$ -catenin.

#### DISCUSSION

Serum PTH concentrations are progressively increased as renal function declines, and this elevation of PTH plays an important role in both the pathogenesis of bone mineral disease and in the development of various complications in uremia [Muntner et al., 2009]. Recent studies have demonstrated the involvement of PTH in the development of fibrotic disorders, and strategies lowering PTH

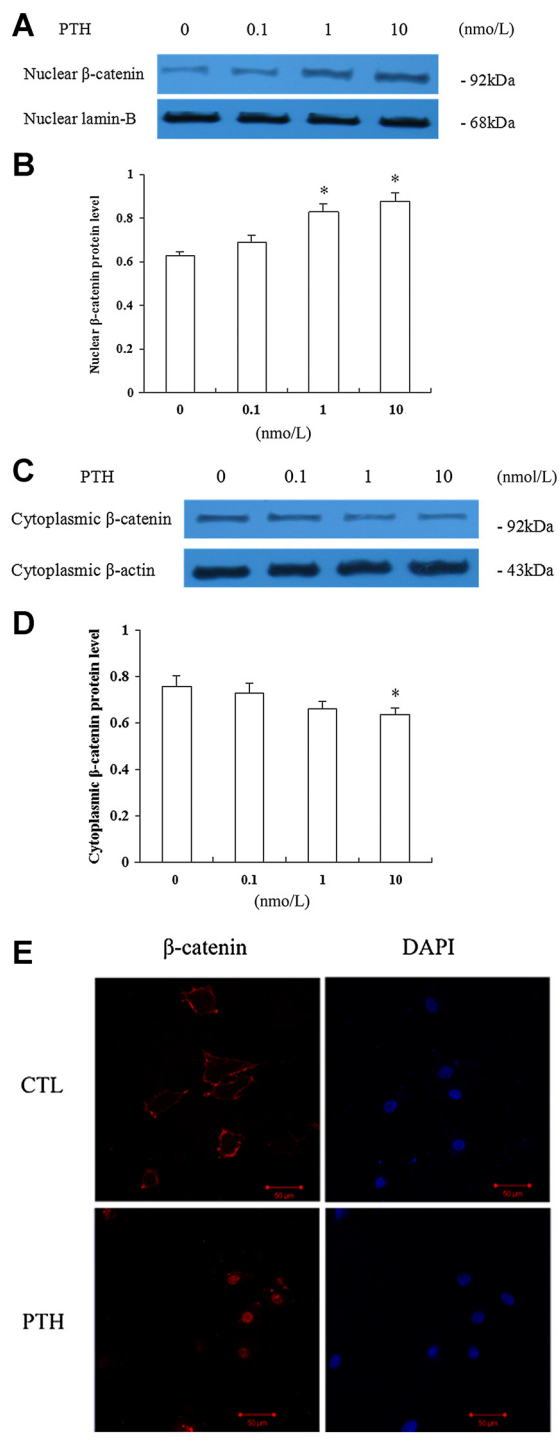


**Fig. 7.** Effect of PTH on nuclear translocation of  $\beta$ -catenin in GECs. Western blotting analyses showed nuclear and cytoplasmic  $\beta$ -catenin abundances after PTH treatment for 48 h as indicated. **A,C:** Representative blots. **B,D:** Graphic presentation. Lamin-B and  $\beta$ -actin were used as internal controls for nuclear and cytoplasmic proteins. The data are expressed as the means  $\pm$  SD. \* $P < 0.05$  versus 0 group. **E:** Immunofluorescent staining of  $\beta$ -catenin (red) in different groups of GECs as indicated. DAPI was used a nuclear stain (blue). Scale bar, 50  $\mu$ m.

levels, including calcimimetics and parathyroidectomy, attenuate the progression of myocardial, vascular and renal tubulointerstitial fibrosis and glomerulosclerosis in CKD animal models [Ogata et al., 2003; Piecha et al., 2008; Guo et al., 2011; Rutledge et al., 2013]. These findings strongly suggest a role of elevated PTH in the fibrotic process. As a hallmark of CKD, endothelial injury is considered to be a critical element in the development of renal fibrosis [Guerrot et al., 2012]. The glomerular endothelium is located at the interface between the glomerular mesangium and blood compartment, without the interposition of the glomerular basement membrane, and this unique structure allows the GECs to serve as targets of metabolic, biochemical and hemodynamic signals that regulate

glomerular microcirculation [Jaimes et al., 2010]. Recent studies by Rashid et al. [2007a,b, 2008] demonstrate that PTH can induce endothelial damage in cultured human umbilical vein endothelial cells. However, to the best of our knowledge, the effect of super physiological PTH on human GECs has not been investigated to date. In the present study, we demonstrated that high PTH could induce phenotypical alterations in primary human GECs: the exposure of human GECs to a high level of PTH resulted in visible changes from a cobblestone-like to a spindle-shaped morphology (Fig. 6). Moreover, we found that increased PTH induced the down-regulation of endothelial marker CD31 and a up-regulation of mesenchymal markers FSP1 and  $\alpha$ -SMA in concentration- and time-dependent

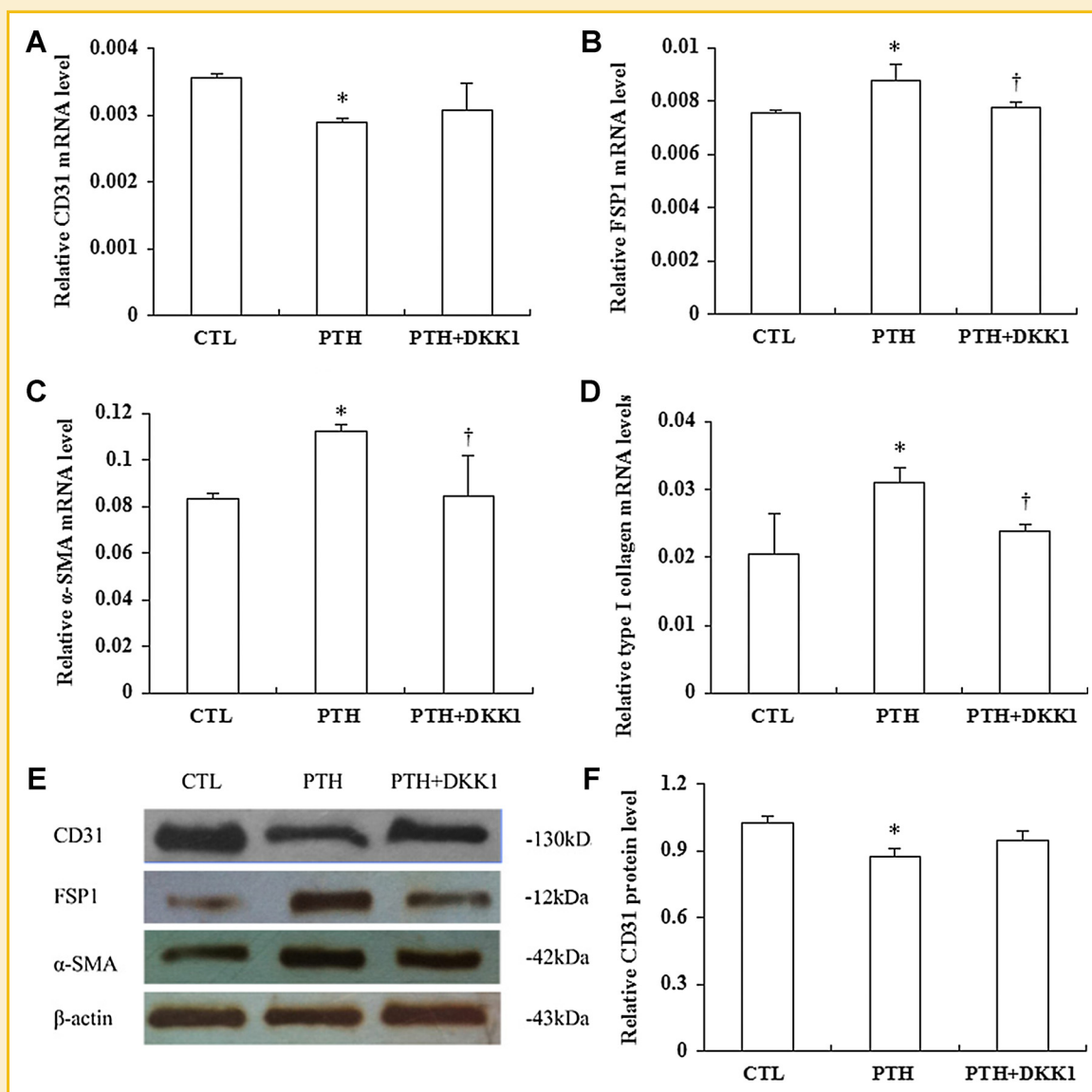


Fig. 8. DKK1 blocked mRNA and protein expression of EndMT-related markers after PTH treatment in GECs. A–D: Real-time PCR analyses showed mRNA expression of CD31 (A), FSP1 (B),  $\alpha$ -SMA (C), and type I collagen (D) after various treatments for 48 h with 100 nmol/L PTH with or without 500 ng/ml DKK1 as indicated. E–J: Western blotting analyses showed protein expression of CD31, FSP1,  $\alpha$ -SMA and type I collagen after various treatments for 48 h with 100 nmol/L PTH with or without 500 ng/ml DKK1 as indicated. E, I: Representative blots. F, G, H, J: Graphic presentation. The data are expressed as the means  $\pm$  SD. \* $P$  < 0.05 versus CTL group; † $P$  < 0.05 versus PTH group. CTL, control; PTH, parathyroid hormone.



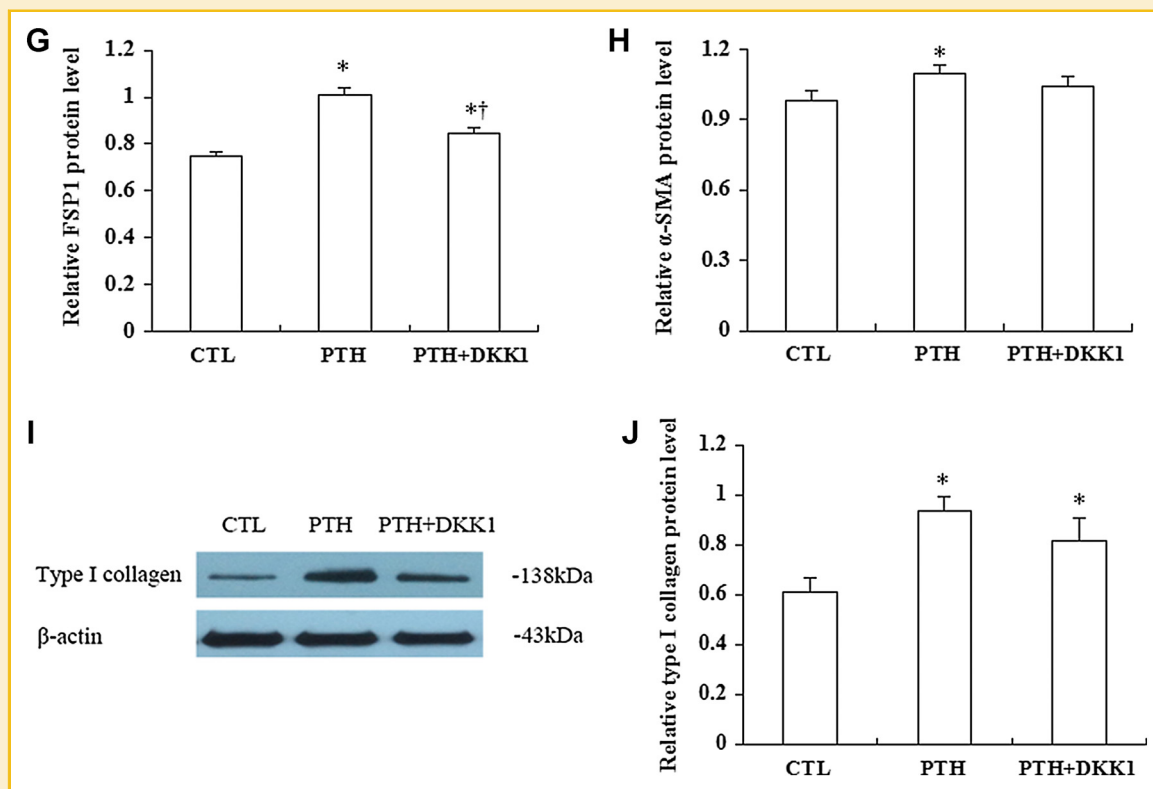


Fig. 8. (Continued)

manner (Fig. 2–4), indicating the effect of PTH on EndMT in GECs. It is noted that the mesenchymal markers responded more quickly than the endothelial markers both in mRNA and protein levels. As EndMT is known to be a dynamic process, these findings suggested an intermediate stage whereby endothelial cells display markers of their parental origin as well as those of emerging mesenchymal features. Considering the important role of EndMT in fibrotic disorders, this PTH-induced phenotypic change in GECs might possibly represent a mechanism involved in kidney fibrosis in CKD.

Despite the increasing evidence of the existence and contribution of EndMT in such pathologies, the underlying molecular details remain unclear. In addition to the well-known TGF- $\beta$  signal [Zeisberg et al., 2007; Li et al., 2010, 2011; Medici et al., 2011], recent studies have provided evidence implicating canonical Wnt signaling in EndMT. The nuclear translocation of  $\beta$ -catenin has been demonstrated to be the key element in the activation of the canonical Wnt pathway. Liebner et al. [2004] found that  $\beta$ -catenin is required for EndMT during heart cushion development in the embryonic mouse. Using the reporter mouse line TOPGAL, Aisagbonhi et al. [2011] demonstrated that  $\beta$ -catenin-dependent canonical Wnt signaling directly induced EndMT in cardiac fibrosis after myocardial infarction. Moreover, Maddaluno et al. [2013] reported that increased  $\beta$ -catenin nuclear translocation may also be implicated in EndMT during the progression of cerebral cavernous malformation (CCM). However, little is known regarding the involvement of  $\beta$ -catenin nuclear translocation in renal EndMT. Our data showed that PTH induced EndMT in GECs, which was accompanied by the nuclear

translocation of  $\beta$ -catenin. Furthermore, blockage of  $\beta$ -catenin nuclear translocation with the specific inhibitor DKK1 could partially attenuate the EndMT induced by PTH in GECs (Figs. 7 and 8). These findings strongly suggested the crucial role of canonical Wnt signaling activation in PTH-induced EndMT in human GECs. A further understanding of the  $\beta$ -catenin-dependent Wnt pathway in EndMT might lead to a novel therapeutic target for renal fibrosis.

In summary, the present study demonstrated that increased PTH induced EndMT in primary human GECs and that the phenotypic alteration was partially mediated by the nuclear translocation of  $\beta$ -catenin. These results suggested that early intervention for increased PTH might be beneficial in delaying the progression of renal fibrosis in CKD.

## ACKNOWLEDGMENTS

These studies were supported by grants from the National Natural Science Foundation of China (Key Program 81130010, 81370919) and Natural Science Foundation of Jiangsu Province (BK 2011603, BK 2012751).

## REFERENCES

Aisagbonhi O, Rai M, Ryzhov S, Atria N, Feoktistov I, Hatzopoulos AK. 2011. Experimental myocardial infarction triggers canonical Wnt signaling and endothelial-to-mesenchymal transition. *Dis Model Mech* 4:469–483.

- Bevan HS, Slater SC, Clarke H, Cahill PA, Mathieson PW, Welsh GI, Satchell SC. 2011. Acute laminar shear stress reversibly increases human glomerular endothelial cell permeability via activation of endothelial nitric oxide synthase. *Am J Physiol Renal Physiol* 301:F733–F742.
- Greka A, Mundel P. 2012. Cell biology and pathology of podocytes. *Annu Rev Physiol* 74:299–323.
- Grutzmacher C, Park S, Zhao Y, Morrison ME, Sheibani N, Sorenson CM. 2013. Aberrant production of extracellular matrix proteins and dysfunction in kidney endothelial cells with a short duration of diabetes. *Am J Physiol Renal Physiol* 304:F19–F30.
- Guerrero D, Dussaule JC, Kavvadas P, Boffa JJ, Chadjiachristos CE, Chatziantoniou C. 2012. Progression of renal fibrosis: The underestimated role of endothelial alterations. *Fibrogenesis Tissue Repair Suppl* 1:S15.
- Guo Y, Yuan W, Wang L, Shang M, Peng Y. 2011. Parathyroid hormone-potentiated connective tissue growth factor expression in human renal proximal tubular cells through activating the MAPK and NF- $\kappa$ B signaling pathways. *Nephrol Dial Transplant* 26:839–847.
- Hashimoto N, Phan SH, Imaizumi K, Matsuo M, Nakashima H, Kawabe T, Shimokata K, Hasegawa Y. 2010. Endothelial-mesenchymal transition in bleomycin-induced pulmonary fibrosis. *Am J Respir Cell Mol Biol* 43:161–172.
- Izawa-Ishizawa Y, Ishizawa K, Sakurada T, Imanishi M, Miyamoto L, Fujii S, Taira H, Kihira Y, Ikeda Y, Hamano S, Tomita S, Tsuchiya K, Tamaki T. 2012. Angiotensin II receptor blocker improves tumor necrosis factor- $\alpha$ -induced cytotoxicity via antioxidative effect in human glomerular endothelial cells. *Pharmacology* 90:324–331.
- Jaimes EA, Hua P, Tian RX, Raji L. 2010. Human glomerular endothelium: Interplay among glucose, free fatty acids, angiotensin II, and oxidative stress. *Am J Physiol Renal Physiol* 298:F125–F132.
- Jefferson JA, Alpers CE, Shankland SJ. 2011. Podocyte biology for the bedside. *Am J Kidney Dis* 58:835–845.
- Landray MJ, Wheeler DC, Lip GY, Newman DJ, Blann AD, McGlynn FJ, Ball S, Townend JN, Baigent C. 2004. Inflammation, endothelial dysfunction, and platelet activation in patients with chronic kidney disease: The chronic renal impairment in Birmingham (CRIB) study. *Am J Kidney Dis* 43:244–253.
- Li Z, Jimenez SA. 2011. Protein kinase C  $\delta$  and the c-Abl kinase are required for transforming growth factor- $\beta$  induction of endothelial-mesenchymal transition in vitro. *Arthritis Rheum* 63:2473–2483.
- Li J, Qu X, Bertram JF. 2009. Endothelial-myofibroblast transition contributes to the early development of diabetic renal interstitial fibrosis in streptozotocin-induced diabetic mice. *Am J Pathol* 175:1380–1388.
- Li J, Qu X, Yao J, Caruana G, Ricardo SD, Yamamoto Y, Yamamoto H, Bertram JF. 2010. Blockade of endothelial-mesenchymal transition by a Smad3 inhibitor delays the early development of streptozotocin-induced diabetic nephropathy. *Diabetes* 59:2612–2624.
- Liebner S, Cattelino A, Gallini R, Rudini N, Lurlaro M, Piccolo S, Dejana E. 2004.  $\beta$ -Catenin is required for endothelial-mesenchymal transformation during heart cushion development in the mouse. *J Cell Biol* 166:359–367.
- Liu Y. 2011. Cellular and molecular mechanism of renal fibrosis. *Nat Rev Nephrol* 7:684–696.
- Loncar G, Bozic B, Dimkovic S, Prodanovic N, Radojicic Z, Cvorovic V, Dimkovic S, Popovic-Brkic V. 2011. Association of increased parathyroid hormone with neuroendocrine activation and endothelial dysfunction in elderly men with heart failure. *J Endocrinol Invest* 34:e78–e85.
- Medici D, Potenta S, Kalluri R. 2011. Transforming growth factor- $\beta$ 2 promotes Snail-mediated endothelial-mesenchymal transition through convergence of Smad-dependent and Smad-independent signaling. *Biochem J* 438:515–520.
- Maddaluno L, Rudini N, Cuttano R, Bravi L, Giampietro C, Corada M, Ferrarini L, Orsenigo F, Papa E, Boulday G, Tournier-Lasserre E, Chapon F, Richichi C, Retta SF, Lampugnani MG, Dejana E. 2013. EndMT contributes to the onset and progression of cerebral cavernous malformations. *Nature* 498:492–496.
- Muntner P, Jones TM, Hyre AD, Melamed ML, Alper A, Raggi P, Leonard MB. 2009. Association of serum intact parathyroid hormone with lower estimated glomerular filtration rate. *Clin J Am Soc Nephrol* 4:186–194.
- Nagasu H, Satoh M, Kidokoro K, Nishi Y, Channon KM, Sasaki T, Kashiwara N. 2012. Endothelial dysfunction promotes the transition from compensatory renal hypertrophy to kidney injury after unilateral nephrectomy in mice. *Am J Physiol Renal Physiol* 302:F1402–F1408.
- Nakagawa T, Sato W, Glushakova O, Heinig M, Clarke T, Campbell-Thompson M, Yuzawa Y, Atkinson MA, Johnson RJ, Croker B. 2007. Diabetic endothelial nitric oxide synthase knockout mice develop advanced diabetic nephropathy. *J Am Soc Nephrol* 18:539–550.
- Ogata H, Ritz E, Odoni G, Amann K, Orth SR. 2003. Beneficial effects of calcimimetics on progression of renal failure and cardiovascular risk factors. *J Am Soc Nephrol* 14:959–967.
- Piecha G, Kokeny G, Nakagawa K, Koleganova N, Geldyyev A, Berger I, Ritz E, Schmitt CP, Gross ML. 2008. Calcimimetic R-568 or calcitriol: Equally beneficial on progression of renal damage in subtotal nephrectomized rats. *Am J Physiol Renal Physiol* 294:F748–F757.
- Rashid G, Bernheim J, Green J, Benchetrit S. 2007a. Parathyroid hormone stimulates the endothelial nitric oxide synthase through protein kinase A and C pathways. *Nephrol Dial Transplant* 22:2831–2837.
- Rashid G, Bernheim J, Green J, Benchetrit S. 2007b. Parathyroid hormone stimulates endothelial expression of atherosclerotic parameters through protein kinase pathways. *Am J Physiol Renal Physiol* 296:F60–F66.
- Rashid G, Bernheim J, Green J, Benchetrit S. 2008. Parathyroid hormone stimulates the endothelial expression of vascular endothelial growth factor. *Eur J Clin Invest* 38:798–803.
- Rieder F, Kessler SP, West GA, Bhilocha S, de la Motte C, Sadler TM, Gopalan B, Stylianou E, Fiocchi C. 2011. Inflammation-induced endothelial-to-mesenchymal transition a novel mechanism of intestinal fibrosis. *Am J Pathol* 179:2660–2673.
- Rutledge MR, Farah V, Adebayo AA, Seawell MR, Bhattacharya SK, Weber KT. 2013. Parathyroid hormone, a crucial mediator of pathologic cardiac remodeling in aldosteronism. *Cardiovasc Drugs Ther* 27:161–170.
- Sun YB, Qu X, Zhang X, Caruana G, Bertram JF, Li J. 2013. Glomerular endothelial cell injury and damage precedes that of podocytes in adriamycin-induced nephropathy. *Plos ONE* 8:e55027.
- Tang RN, Lv LL, Zhang JD, Dai HY, Li Q, Zheng M, Ni J, Ma KL, Liu BC. 2013. Effects of angiotensin II receptor blocker on myocardial endothelial-to-mesenchymal transition in diabetic rats. *Int J Cardiol* 162:92–99.
- Theilade S, Lajer M, Jorsal A, Tarnow L, Parving HH, Rossing P. 2012. Arterial stiffness and endothelial dysfunction independently and synergistically predict cardiovascular and renal outcome in patients with type 1 diabetes. *Diabet Med* 29:990–994.
- Weil EJ, Lemley KV, Mason CC, Yee B, Jones LI, Blouch K, Lovato T, Richardson M, Myers BD, Nelson RG. 2012. Podocyte detachment and reduced glomerular capillary endothelial fenestration promote kidney disease in type 2 diabetic nephropathy. *Kidney Int* 82:1010–1017.
- Zeisberg EM, Tarnavski O, Zeisberg M, Dorfman AL, McMullen JR, Gustafsson E, Chandraker A, Yuan X, Pu WT, Roberts AB, Neilson EG, Sayegh MH, Izumo S, Kalluri R. 2007. Endothelial-to-mesenchymal transition contributes to cardiac fibrosis. *Nat Med* 13:952–961.
- Zeisberg EM, Potenta SE, Sugimoto H, Zeisberg M, Kalluri R. 2008. Fibroblasts in kidney fibrosis emerge via endothelial-to-mesenchymal transition. *J Am Soc Nephrol* 19:2282–2287.